Tubulin Polyglutamylase: Partial Purification and Enzymatic Properties†

Catherine Regnard,* Stéphane Audebert, Élisabeth Desbruyères, Philippe Denoulet, and Bernard Eddé

Laboratoire de Biochimie Cellulaire, CNRS UPR 9065 and Université P. et M. Curie, Collège de France, 11 place Marcelin Berthelot, 75005 Paris, France

Received February 20, 1998; Revised Manuscript Received April 9, 1998

ABSTRACT: In this work, we report on a novel enzyme, tubulin polyglutamylase, which catalyzes the posttranslational formation of polyglutamyl side chains onto α- and β-tubulin. The length of the polyglutamyl side chain regulates the interaction between tubulin and various microtubule-associated proteins. We first developed an in vitro glutamylation assay. Activity measured in brain, a tissue particularly enriched with glutamylated tubulin, decreases during postnatal development. Thus, brains from 3-day-old mice were chosen as the starting material, and the enzyme was purified ∼1000-fold. Its M_r was estimated to be 360K and its sedimentation coefficient 10 s. The enzyme catalyzes the MgATP-dependent addition of L-glutamate onto tubulin subunits. Microtubules are much better substrates than unpolymerized tubulin, and the reaction is very specific for glutamate, other amino acids or glutamate analogues not being substrates. Moreover, glutamyl units are added sequentially onto tubulin, leading to progressive elongation of the polyglutamyl side chains. Side chains of one to six or seven glutamyl units were obtained with microtubules, whereas much longer side chains (up to 15−20 units) were formed with unpolymerized tubulin. Interestingly, such very long polyglutamyl side chains were recently detected in some situations in vivo.

Microtubules (MTs[1]), alone or as a part of complex structures, are implicated in numerous cellular functions such as cell division, directed intracellular transport, dynamic organization of cell morphology, or cilia and flagella beating. The structural unit of MTs, the αβ-tubulin heterodimer, is characterized by a great polymorphism, particularly in the C-terminal domain of each subunit which is exposed on the surface of the MT lattice and implicated in interactions with microtubule-associated proteins (MAPs) (*1*−*5*). α- and β-tubulin are encoded by a multigene family (for review, see ref *6*) and are targets for various posttranslational modifications (PTMs; for a recent review, see ref *7*). Some of these PTMs, such as acetylation and phosphorylation, are shared with other proteins, but others, specific for tubulin, are reported, for instance, the reversible excision of the C-terminal tyrosine of α-tubulin as well as formation of tubulin isoforms lacking the penultimate glutamate residue (Δ2-tubulin). Moreover, we and others have characterized new PTMs, consisting of the addition of either polyglutamyl or polyglycyl side chains of various lengths onto α- and β-tubulin.

Polyglutamylation was first identified in neuronal tubulin and is the main cause of its high isoelectric heterogeneity. Almost 90% of α-tubulin, >85% of class III β-tubulin, and the vast majority of class II β-tubulin are glutamylated, with side chains ranging from one to six or seven glutamyl units in length (*8*−*10*). The first unit of the side chain is linked via an amide bond to the γ-carboxylic group of a glutamate residue near the C terminus. Within the side chain, either γ- or α-linkages were found for α-tubulin, but α-bonds are largely predominant (*11*−*13*).

Immunodetection with a specific mAb, GT335 (*14*), revealed that polyglutamylation is a widespread modification of tubulin from protozoa (*15*) to differentiated cells in metazoa, especially neurons and spermatozoa. In mouse spermatids and spermatozoa, centrioles and flagella are decorated while MTs of the manchette are not (*16*). Interestingly, in HeLa, KE37, and 3T3 cells, a limited but significant immunoreactivity associated with centrosomes, mitotic spindles, and midbodies is observed (*17*).

Polyglutamylation appears to play crucial roles in MT functions. Very low concentrations of anti-polyglutamylated tubulin mAbs (GT335 and B3) completely inhibit flagellar motility (*18*). Recent data also indicate that α- and β-tubulin polyglutamylation regulates the interaction between tubulin and structural MAPs, like the neuronal Tau and MAP2 (*4*), or motor MAPs such as rat kinesin and *Drosophila* nonclaret disjunctional motor domains (*5*).

Experiments performed with neurons in primary culture revealed that the glutamylation reaction is reversible in vivo. Moreover, interesting properties of the reaction were pointed out. In particular, glutamylation is very sensitive to microtubule-depolymerizing drugs, suggesting that MTs are much better substrates than heterodimeric tubulin (*19*).

† This work was supported by the Centre National de la Recherche Scientifique and by the Association Française contre la Myopathie. C.R. was supported by a fellowship from La Fondation pour la Recherche Médicale.

* Corresponding author. Phone: (33) 1 44 27 13 03. Fax: (33) 1 44 27 13 09. E-mail: regnard@ext.jussieu.fr.

[1] Abbreviations: MT, microtubule; MAP, microtubule-associated protein; mAb, monoclonal antibody; PTM, posttranslational modification; Tris, tris(hydroxymethyl)aminomethane; DTT, dithiothreitol; MES, 2-(*N*-morpholino)ethanesulfonic acid; CHES, 2-(*N*-cyclohexylamino)-2-hydroxy-1-propanesulfonic acid; PIPES, piperazine-*N*,*N*′-bis(2-ethanesulfonic acid); PAGE, polyacrylamide gel electrophoresis; HPLC, high-performance liquid chromatography; BICINE, *N*,*N*-bis(2-hydroxyethyl)glycine; TX-100, Triton X-100.

S0006-2960(98)00413-9 CCC: $15.00
Published on Web 06/09/1998

To further investigate the role of tubulin polyglutamylation, a better understanding of the enzymatic mechanisms involved in this process is needed. In this report, we describe the partial purification (~1000-fold) of tubulin polyglutamylase from brains of 3-day-old mice and some unusual properties of this modification.

EXPERIMENTAL PROCEDURES

Tubulin Polyglutamylase Assay. Enzyme activity was measured by incorporation of [^{3}H]glutamate into tubulin, at pH 6.8 or 8.7. Under standard assay conditions at pH 8.7, reaction mixtures (20−100 μL) contained 50 mM Tris (pH 9.0), 2 mM ATP (equilibrated to pH 7 with NaOH), 8 mM $MgCl_2$, 2.5 mM DTT, 10 μM taxotere, L-[^{3}H]glutamate (45−55 Ci/mmol, Amersham), and unlabeled L-glutamate at variable concentrations [0.1 M stock solution in 0.1 M CHES (pH 10)]. In some cases, radioactive glutamate was concentrated under speed vacuum. The reaction mixture was warmed before the addition of 0.1 mg/mL taxotere-stabilized MTs, and the mixture was incubated at 30 °C for 30 min. Standard assay conditions at pH 6.8 were identical to those mentioned above, except that 50 mM PIPES (pH 7.0) was used instead of Tris and the incubation time was longer (2−3 h) because, at limiting glutamate concentrations, incorporation rates are lower at this pH. The reaction was stopped by the addition of Laemmli sample buffer (*20*) and submitted to SDS−PAGE (8 cm long, 1.5 mm thick slab gels). After transfer onto nitrocellulose (*21*) and staining with Ponceau red, α- and β-tubulin bands were cut out and submitted to scintillation counting with 6 mL of Ultima Gold MV (Packard, Groningen, The Netherlands). Background values (15−20 cpm) were subtracted. The signal was linear till 4 μg of loaded tubulin. When the reaction was performed with very low MT concentrations, exogenous nonradioactive tubulin was added to the sample before SDS−PAGE. When rapid results were required, e.g., during the time course of the enzyme purification, the reaction was stopped by the addition of 5 volumes of 5% (w/v) trichloroacetic acid and 10 mM glutamate, and the mixture was filtered under vacuum onto nitrocellulose. After being extensively washed with 1% (v/v) acetic acid, the nitrocellulose sheet was stained with Ponceau red. Slots were then cut out and incubated with 0.1 M NaOH (0.5 mL) for at least 10 min, and Ultima Gold MV (6 mL) was added for counting. The counting efficiency for tritium was 43% (Kontron apparatus) with liquid samples but lower with nitrocellulose sheets. When glutamate incorporation had to be expressed in molar quantities, nitrocellulose sheets were dissolved in 5 mL of Filter-count (Packard) to increase the counting efficiency.

Tubulin Purification and Preparation of Stable MTs. Mouse brain tubulin was purified by phosphocellulose chromatography as described by Paturle-Lafanechère et al. (*22*). Taxotere-stabilized MTs from mouse brain and from HeLa cells were polymerized in the presence of 1 mM GTP and 20 μM taxotere as described by Vallee (*23*). They were carefully resuspended at a concentration of ~10 mg/mL in warm 50 mM MES (pH 6.6), 1 mM EGTA, 1 mM $MgCl_2$, 0.1 mM GTP, and 20 μM taxotere and stored as small aliquots at −80 °C. MT stability under assay conditions was assessed by two independent methods. First, the proportion of sedimentable tubulin was quantified after centrifugation at either 50000*g* for 30 min in a 50 Ti rotor (Beckman) or 20 psi for 10 min in an A100 Airfuge rotor (Beckman). The second method was based on immunofluorescence visualization of MTs (*24*). Briefly, the MT samples were diluted to 0.04 mg/mL, cross-linked with 0.75% glutaraldehyde, centrifuged on glass coverslips, and processed for immunofluorescence using the anti-α-tubulin mAb DM1A (Amersham) and fluoresceine-conjugated anti-mouse IgG secondary antibodies (Biosys). The length and density of MTs were visualized on photomicrographs. Microtubles purified from HeLa cells appeared to be shorter (~2 μm) than those purified from brain (5−10 μm). No obvious difference was observed between freshly prepared and long-term stored MTs.

Purification of Tubulin Polyglutamylase. A typical purification procedure is summarized in Table 1. All steps, except step 5, were carried out at 0−4 °C. A protease inhibitor cocktail [aprotinin, leupetin, and 4-(2-aminoethyl)-benzenesulfonyl fluoride each at 10 μg/mL] was added to all buffers and samples, except the chromatography and dialysis buffers.

Step 1. Brains from 3-day-old mice were taken rapidly and homogenized in a glass−Teflon Potter with 3 mL/g of tissue of buffer B [50 mM BICINE (pH 9.0), 1 mM EGTA, 1 mM $MgCl_2$, 0.01% TX-100, and 1 mM DTT]. After 10 strokes at 1200 rpm, NaCl and TX-100 were added to final concentrations of 0.13 M and 0.1%, respectively. The extract was homogenized again and centrifuged (70000*g* for 45 min), and the pellet was re-extracted with the same buffer (1.5 mL/g of tissue). The two supernatants were pooled to yield fraction I.

Step 2. Fraction I was loaded, at a flow rate of 30 mL cm^{-2} h^{-1}, onto a freshly prepared phosphocellulose column (45 mL of gel per gram of protein) equilibrated in buffer B containing 0.1 M NaCl. The column was then washed with 3 column volumes of the same buffer, at a flow rate of 60 mL cm^{-2} h^{-1}. A linear gradient was developed from 0.1 to 0.5 M NaCl in 5 column volumes, followed by a 1 M NaCl final step. Active fractions were pooled (fraction II).

Step 3. Fraction II was dialyzed overnight (Spectra/Por 2, Spectrum) against buffer T [10 mM Tris (pH 8.7), 1 mM EGTA, 1 mM $MgCl_2$, 1 mM DTT, and 0.01% TX-100], cleared by centrifugation (75000*g* for 30 min), diluted to 0.4−0.6 mg/mL, and submitted to $MgCl_2$ precipitation. A 20 mM $MgCl_2$ solution in buffer T was slowly added (~30 min) under continuous stirring to a final concentration of 6 mM. After 15 min, the sample was centrifuged in an SW27 rotor (50000*g* for 30 min). Pellets were resuspended in $\sim^1/_{10}$ of the volume of the supernatant (giving a protein concentration of ~1 mg/mL) in buffer T without $MgCl_2$ and homogenized in a glass−Teflon Potter. Sodium citrate at 0.16 M was then added under slow stirring to improve solubilization of the pellet. Precipitation was then triggered by increasing the sodium citrate concentration progressively up to 0.7 M. After centrifugation (12000*g* for 20 min), the pellet was dissolved so that it would be as concentrated as possible (3−5 mg/mL) in buffer M [50 mM MES (pH 6.8), 1 mM EGTA, 1 mM $MgCl_2$, 1 mM DTT, and 0.01% TX-100] containing 0.35 M NaCl and clarified (50000*g* for 30 min) to yield fraction III.

Step 4. Fraction III was submitted to centrifugation (SW27 rotor, 100000*g* for 66 h) on a linear 10 to 18% sucrose gradient in buffer M containing 0.35 M NaCl. Proteins (4.5 mg) were loaded onto each gradient tube (38 mL). Fractions

Table 1: Purification of Tubulin Polyglutamylase from Brains of 3-Day-Old Mice

fraction	purification step	volume (mL)	protein concentration (mg/mL)	protein amount (mg)	specific activity (cpm/μg)[a]	purification (-fold)	yield (%)
I	extraction	190	11	2090	22	1	100
II	phosphocellulose chromatography	57	1.4	80	470	21	82
III	$MgCl_2$ and sodium citrate precipitation	4.5	3	13.5	1200	55	35
IV	sucrose gradient sedimentation	0.6	2	1.2	8600	391	22
V	size-exclusion chromatography	0.2	1.2	0.24	20000	910	10

[a] Enzyme assays were performed under standard conditions at pH 8.7, in the presence of 6 μM [^{3}H]glutamate. Specific activities were expressed as counts per minute incorporated into α- and β-tubulin, relative to the amount of protein present in each fraction.

of 2 mL were collected with a peristaltic pump at a flow rate of 4 mL/min. Protein standards (albumin, aldolase, catalase, cytochrome *c*, β-galactosidase, hemoglogin, thyroglobulin, and transferrin) used for determination of the sedimentation coefficient were detected by OD at 415 and 280 nm. Active fractions were pooled and concentrated to 2−3 mg/mL on Centriprep C50 apparatus (cutoff of 50 000, Amicon) and clarified (50000*g* for 10 min), yielding fraction IV.

Step 5. Fractionation by size-exclusion HPLC (TSK G3000 SW_{XL}, 7.8 × 300 mm, Tosohaas) was performed in buffer M containing 0.25 M NaCl, at room temperature and at a flow rate of 1 mL/min. Fractions (0.3 mL) were collected and immediately cooled in melting ice. Active fractions were concentrated to ∼1 mg/mL by ultrafiltration as before (fraction V) and stored in the presence of 10% glycerol, at −80 °C. Protein standards used for calibration were albumin, catalase, cytochrome *c*, ovalbumin, and thyroglobulin. Care must be taken not to apply ≤1 mg of protein onto this column because the yields decreased markedly with lower amounts.

Cosedimentation of Tubulin Polyglutamylase with MTs. Cosedimentation experiments were developed from standard assay conditions at neutral pH. Fraction V (10−100 μL) was diluted to 1/20 in 33 mM PIPES (pH 7), 6 mM $MgCl_2$, 2 mM ATP, 1 mM EGTA, 1 mM DTT, 2 mM glutamate, 10 μg/mL taxotere, 12.5 mM NaCl, and 0.1 mg/mL MTs. Because of the presence of 250 mM NaCl in fraction V, the total NaCl concentration reached 25 mM. After incubation for 5 min at room temperature, MTs were pelleted (50000*g* for 15 min at 12 °C). The pellet was gently resuspended in 20−200 μL of 100 mM PIPES (pH 7), 6 mM $MgCl_2$, 1 mM ATP, 20 μg/mL taxotere, and 0.01% TX-100 at 4 °C and then adjusted to 125 mM NaCl and centrifuged (50000*g* for 15 min at 4 °C). Under this condition, tubulin polyglutamylase was dissociated from MTs and recovered in the supernatant.

Electrophoresis. SDS−PAGE (*20*) was performed on 8% acrylamide, 0.11% bisacrylamide, slab gels containing 0.1% (w/v) SDS (90% pure, Merck, Darmstadt, Germany). Isoelectric focusing in denaturing 9.5 M urea cylindrical gels was performed as described (*25*), except that pH 5.0−6.0 ampholytes (Serva, Heidelberg, Germany) were used. The second dimension was performed on 24 cm long slab gels as described previously (*26*). Exposures were performed at −80 °C using Kodak (Rochester, NY) XAR-5 films after enhancement with Amplify (Amersham).

Peptide Mapping of in Vitro Glutamylated α*-Tubulin*. The reaction mixture was submitted to SDS−PAGE and transferred onto nitrocellulose, and the α-tubulin bands were cut out. Proteolytic fragments were obtained according to the method described by Aebersold et al. (*27*) by overnight incubation at 37 °C with 125 μg/mL thermolysin (Boehringer, Indianapolis, IN) in 50 mM Tris (pH 8) and 0.1 mM $CaCl_2$. The resulting peptides were analyzed by HPLC (Waters Millipore, Bedford, MA) using a C18 column (4.6 × 220 mm, Brownlee, Applied Biosystems) at a flow rate of 1 mL/min. Solution A was 0.1% trifluoroacetic acid in water, and solution B was 0.09% trifluoroacetic acid and 70% acetonitrile in water. Peptides were eluted with a linear gradient of 5 to 29% solution B over the course of 40 min. Radioactivity was automatically measured using an in-line flow radioactivity detector (FLO-ONE, Radiomatic, Tampa, FL) placed immediately after the UV densitometer. Characterization of the radioactive peptides was confirmed by coelution of unlabeled synthetic C-terminal α-tubulin peptides bearing zero to two glutamyl units (*22*).

Determination of the Protein Concentration. The protein concentration was measured according to Bradford (*28*) with bovine serum albumin as the standard, using the Bio-Rad (Hercules, CA) reagent.

RESULTS

In Vitro Assay for Tubulin Polyglutamylase. Preliminary experiments had shown that L-[^{3}H]glutamate was incorporated into polymerized tubulin in the presence of MgATP, at pH 8.3−8.7. Although MT depolymerization was expected to occur at this rather alkaline pH, sedimentation experiments and immunofluorescence analysis indicated that most MTs were stable within the 30 min assay period, provided that taxotere (10 μM) and $MgCl_2$ (≥4 mM) were present (not shown). Salts, such as NaCl or KCl, had a strong inhibitory effect on the glutamylation reaction (see below). Protein samples were therefore desalted prior to the assay. When a desalted soluble 3-day-old brain extract was assayed under standard conditions at pH 8.7 and analyzed by SDS−PAGE and fluorography, two major labeled bands migrating as α- and β-tubulin subunits were detected (Figure 1). Incorporated radioactivity was measured, after transfer of a duplicate gel onto nitrocellulose, according to the method developed by Audebert et al. (*19*). Values of 350 and 140 cpm were obtained for α- and β-tubulin, respectively. This labeling could not result from mRNA translation since other major proteins such as actin were not labeled. Whether it corresponds to glutamylation was confirmed by peptide map analysis (see below). Omission of taxotere-stabilized MTs or their replacement by free tubulin heterodimers resulted in a much lower level of labeling (not shown), suggesting a preferential activity of the enzyme toward MTs.

Solubilization of Tubulin Polyglutamylase. Enzyme solubilization from a crude brain extract was shown to depend

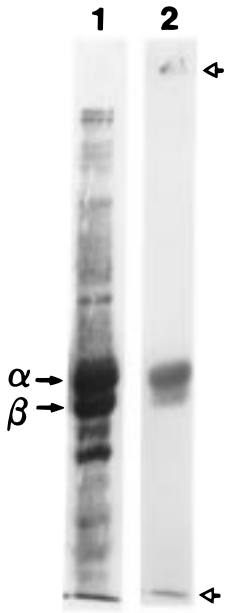

FIGURE 1: Tubulin polyglutamylase activity in soluble brain extract of 3-day-old mice. Desalted soluble brain extract of 3-day-old mice (70000*g* for 45 min at 4 °C) was assayed under standard conditions at pH 8.7, at 1 mg/mL, in the presence of 6 μM [^{3}H]glutamate. After incubation for 30 min at 30 °C, the reaction mixture (25 μL) was analyzed by SDS−PAGE: lane 1, Coomassie blue staining; and lane 2, fluorography (40 day exposure). The two major labeled bands comigrated with α- and β-tubulin subunits (arrows). Faint labeling was also observed at the migration front and at the bottom of the well (arrowheads).

essentially upon pH. Raising the pH of the extraction buffer from 6.6 to 9 increased ~4-fold the amount of soluble activity recovered in the supernatant. Above pH 9.5, the yield dropped abruptly. The presence of TX-100 in the extraction buffer allowed activity measurements in pellet fractions, and thus quantification of the solubilization efficiency. Soluble extracts containing up to 80% of the total activity were obtained by two successive extractions in buffer B (pH 9), 0.13 M NaCl and 0.1% TX-100. Partial solubilization (~50%) could also be achieved at pH 6.6, provided that NaCl (or KCl) was added at concentrations of ≥0.2 M. Either alkaline pH or a high salt concentration was important for maintaining enzyme solubility in active fractions. However, the salt requirement at neutral pH depends on protein concentration (see below).

Partial Purification of Tubulin Polyglutamylase from 3-Day-Old Mouse Brain. Enzyme activity was measured in soluble mouse brain extracts at different stages of postnatal development. It was maximal in day 2−3 after birth, decreased progressively to 20% in day 16, and remained constant thereafter (Figure 2). Thus, brains of 3-day-old mice were used as the starting material for purification. A typical purification procedure of tubulin polyglutamylase is summarized in Table 1. All steps, except when indicated, were performed at 0−4 °C. For this preparation, ~350 brains weighing ~130 mg each were used. Soluble extract (fraction I, Figure 3A, lane 1) was fractionated on a phosphocellulose column. The bulk of the loaded material did not bind to the column, in particular, tubulin which represented almost 20% of the proteins in fraction I (Figure 3A, lanes 1 and 2). Enzymatic activity was recovered in the fractions eluted between 0.19 and 0.30 M NaCl, the peak being at 0.25 M NaCl (fraction II, Figure 3A, lane 3).

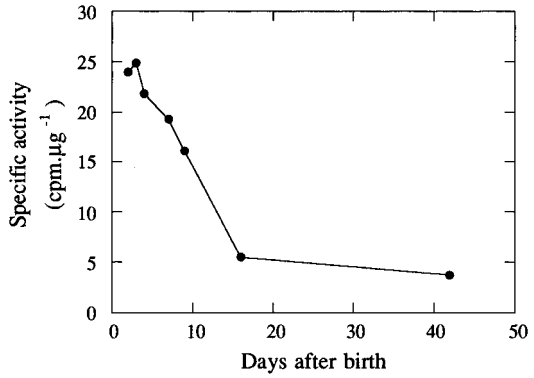

FIGURE 2: Tubulin polyglutamylase activity decreases during postnatal mouse brain development. Desalted soluble extracts from 2-, 3-, 4-, 7-, 9-, 16-, and 42-day-old mouse brains were assayed under standard conditions at pH 8.7, at 1 mg/mL, in the presence of 6 μM [^{3}H]glutamate. Specific activities are expressed as counts per minute (cpm) incorporated into α- and β-tubulin per microgram of soluble proteins added to the assay. The ratio of cpm(α)/cpm-(β) did not vary significantly during development (2.5−3).

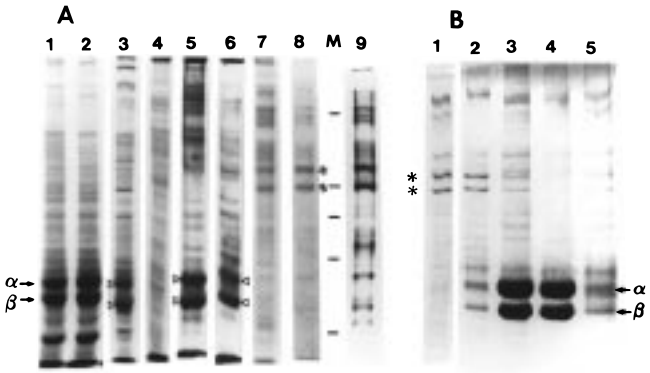

FIGURE 3: SDS−PAGE analysis. (A) Fractions obtained during purification of tubulin polyglutamylase. Fractions are named according to Table 1: lane 1, fraction I (15 μg); lane 2, proteins unbound to the phosphocellulose column (15 μg); lane 3, fraction II (15 μg); lane 4, proteins eluted from the phosphocellulose column at 1 M NaCl (10 μg); lane 5, $MgCl_2$ pellet obtained before sodium citrate precipitation (15 μg); lane 6, fraction III (10 μg); lane 7, fraction IV (5 μg); lane 8, fraction V (2.5 μg); and lane 9, fraction V (1.5 μg). In lanes 1−8, Coomassie blue staining was used ; in lane 9, silver staining was used. Arrows on the left indicate the position of α- and β-tubulin. Note that the two protein bands indicated by arrowheads in fractions II and III (lanes 3, 5, and 6) migrated slightly faster than tubulin subunits. Two proteins (110 and 130 kDa) prominent in fraction V are indicated by asterisks. Electrophoretic positions of myosin (200 kDa), β-galactosidase (116.2 kDa), phosphorylase *b* (97.4 kDa), bovine serum albumin (66.2 kDa), and ovalbumin (42.7 kDa) are indicated under lane M. (B) Cosedimentation of tubulin polyglutamylase with MTs. Similar ratios of each fraction were loaded onto the gel: lane 1, fraction V (100% activity); lane 2, first supernatant containing the proteins not cosedimented with MTs (5% of the initial activity); lane 3, first MT pellet and cosedimented proteins (70% of the initial activity); lane 4, second MT pellet obtained after dissociation at a higher ionic strength (3% of the initial activity); and lane 5, second supernatant containing dissociated proteins and tubulin polyglutamylase activity (50% of the initial activity).

Surprisingly, the enzyme precipitates at low $MgCl_2$ concentrations (Figure 4). Activity in the pellets increased markedly with Mg^{2+} concentrations between 1 and 6 mM. At ≥6 mM, 80% of the activity was recovered in the pellet fractions. However, the yields did not exceed ~60%. $MgCl_2$ precipitation was affected by the protein concentration of fraction II; it did not occur below 0.2 mg/mL and was much

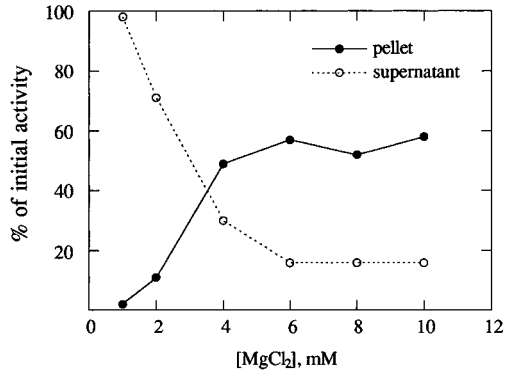

FIGURE 4: Precipitation of tubulin polyglutamylase activity with $MgCl_2$. Fraction II was dialyzed against buffer T, diluted at 0.5 mg/mL, and submitted to $MgCl_2$ precipitation at the indicated concentrations. Pellets were resuspended in buffer T and assayed in parallel with the corresponding supernatants, under standard conditions at pH 8.7, in the presence of 6 μM [^{3}H]glutamate. Results are expressed as the percentage of activity recovered relative to that initially present in fraction II.

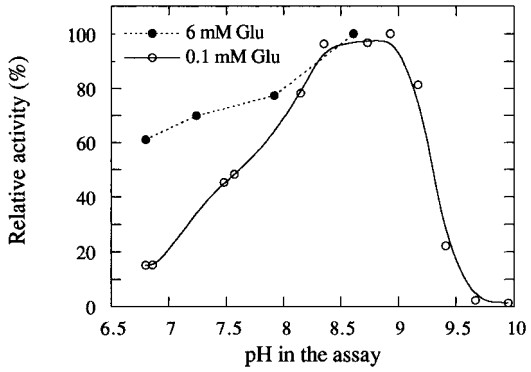

FIGURE 5: pH optimum and glutamate concentration. Fraction IV (40 μg/mL) was assayed under standard conditions using various buffers (50 mM PIPES, MES, Tris, or CHES), in the presence of either 0.1 (○) or 6 mM (●) [^{3}H]glutamate. Indicated pHs were measured at 20 °C in reaction mixtures without proteins. The incubation time was 30 min. Enzymatic activities are expressed as the percentage of the maximum for each glutamate concentration. The ratio cpm(α)/cpm(β) was constant.

less specific above 0.7 mg/mL. It was also prevented in the presence of salts such as NaCl. At 6 mM $MgCl_2$, 12 mM NaCl lowered ~2-fold the precipitation efficiency. For this reason, fraction II was dialyzed overnight against buffer T and diluted to 0.6 mg/mL before we proceeded to the $MgCl_2$ precipitation. Addition of sodium citrate (0.16 M) was necessary to improve solubilization of the precipitate. Thereafter, increasing the sodium citrate concentration to 0.7 M led to precipitation of the enzyme.

The pellet (fraction III, Figure 3A, lane 6) was resuspended in buffer M, containing 0.35 M NaCl, and loaded onto a 10 to 18% linear sucrose gradient. The active fractions, which peaked at 14.5% sucrose, were pooled and concentrated to 2−3 mg/mL by ultrafiltration (yielding fraction IV, Figure 3A, lane 7). The sedimentation coefficient of the enzyme was estimated to be ~10 S, relative to protein standards run in the same experiment. Changing the buffer at this step was crucial because lower yields and peak trailing toward the bottom of the tubes were observed in gradients performed at pH 9 in buffer T or B.

Finally, fraction IV was fractionated by size-exclusion HPLC, at room temperature. Activity was eluted just behind the void volume. The pool of active fractions was concentrated to 1−2 mg/mL, supplemented with 10% glycerol, and stored at −80 °C (fraction V, Figure 3A, lane 8). By comparison with protein standards, the R_s of tubulin polyglutamylase was estimated to be ~70 Å and its M_r 360 000.

It is important to note that enzymatic activity toward α- versus β-tubulin remained in a constant ratio of 2.5−3 in all fractions, indicating that, if distinct enzymes are involved for the glutamylation of each subunit, they were copurified during the purification procedure.

Fraction V displayed ≥20 proteins, as revealed by silver staining (Figure 3A, lane 9). Minor species of ~300−400 kDa were detected, but their intensity did not follow the variation of the enzymatic activity in the fractions obtained by size-exclusion chromatography (not shown). On the other hand, the two major proteins in fractions V (110 and 130 kDa) which could be implicated in an oligomeric complex were separated from enzymatic activity in cosedimentation experiments with MTs. In these experiments, numerous parameters had to be meticulously determined to ensure at one and the same time the stability of MTs, the intrinsic solubility of tubulin polyglutamylase, and the stability of its activity without preventing interaction with microtubules. This was achieved by diluting fraction V to 1/20 in PIPES buffer (pH 7) to lower both salt and protein concentrations (see Experimental Procedures) and by working at 12 °C. Thus, in the absence of MTs, the enzyme remained almost entirely soluble, whereas after incubation with taxotere-stabilized MTs, ~75% of the initial activity cosedimented. In contrast, most of the 110 and 130 kDa proteins remained in the supernatant with only ~5% of the initial activity (Figure 3B, lanes 1−3). The enzyme was then dissociated from MTs by increasing PIPES and NaCl concentrations from 33 to 100 mM and from 25 to 125 mM, respectively. The final supernatant contained ~50% of the initial activity and numerous proteins, among which that (or those) corresponding to tubulin polyglutamylase cannot be identified (Figure 3B, lane 4−5).

Enzyme Stability. Concentrated fractions IV and V were stable for several months when stored at −80 °C in the presence of 10% glycerol. However, incubation of fraction IV in buffer T at pH 8.7 for 1 h led to a 50% loss of activity at 20 °C and 75% at 30 °C. At 30 °C, the loss was reduced to 40% in the presence of 0.1 mg/mL MTs, while neither bovine serum albumin nor the other substrates, ATP or glutamate, had any protecting effect. Similar experiments performed at pH 6.8 did not show any significant loss of activity within 3 h of incubation. Consistent with these observations, the period of constant incorporation rate was longer at pH 6.8 than at pH 8.7.

pH Optimum and Glutamate Concentration. The pH optimum of tubulin polyglutamylase activity was first determined in the presence of 0.1 mM glutamate using buffers ranging in pH between 6.8 and 10 (Figure 5). Activity increased markedly with the pH going from 6.8 to 8.3, with a large optimum between 8.3 and 8.9, and then decreased sharply. At physiological pH, the activity was 15% of the maximal level. However, when the glutamate concentration was raised to 6 mM, the activity was less dependent on pH, decreasing by only 40% between pH 8.7 and 6.8 (Figure 5). For this reason, we investigated the influence of pH on the enzymatic parameters of glutamate.

When activity was tested at various glutamate concentrations, hyperbolic curves were obtained, fitting well with the Michaelis−Menten model and giving K_m(Glu) values of ∼3 and ∼0.8 mM at pH 6.8 and 8.7, respectively. On the other hand, the V_m was similar at both pHs. This suggests that the high pH optimum observed at low glutamate concentrations is a result of the free amine of glutamate (pK = 9.7 at 25 °C) being the substrate for the reaction.

Specificity for L*-Glutamate and ATP*. Other amino acids (D-Glu, L-Asp, L-Gln, L-Asn, L-Ser, L-Lys, L-Leu, and L-Gly) or glutamate analogues (αGlu-Glu, γGlu-Glu, Iso-Gln, *N*-acetyl-Glu, norvaline, GABA, and Gla) were tested for their capacity to inhibit the glutamylation reaction or to be incorporated in place of or together with L-glutamate. These assays were performed at pH 8.7 under the standard conditions so that the concentration of the potential competitor (10 mM) was nearly 1000-fold higher than that of [^{3}H]-glutamate (12 μM). Under these conditions, we calculated that >20% inhibition would be obtained with a K_I of <40 mM for competitive and noncompetitive inhibition and with a K_I of <66 mM for uncompetitive inhibition. None of the compounds tested affected glutamate incorporation by ≥15%, indicating a high specificity of tubulin polyglutamylase for L-glutamate.

In the presence of 3 mM Glu, at pH 8.7, the apparent K_m-(ATP) was ∼0.1 mM. UTP, CTP, or GTP could not replace ATP in the assay, even with very low efficiency. Mg^{2+} was absolutely required with an optimal concentration of 6−8 mM.

Inhibition by Salts. Monovalent cations above 5−10 mM strongly inhibited the glutamylation reaction. For instance, 40 and 80 mM NaCl or KCl provoked ∼50 and ∼90% inhibition, respectively. Sodium acetate was less inhibitory (50% inhibition at 100 mM). Sodium sulfate and citrate had stronger effects leading to ∼90% inhibition at 20 mM (40 mM Na^+) and 10 mM (30 mM Na^+), respectively. These results illustrate why samples of low specific activity must be desalted before being assayed.

Tubulin Substrate. Experiments performed at various tubulin concentrations confirmed that MTs are better substrates than unpolymerized tubulin. At saturating tubulin concentrations, maximum incorporation was ∼4-fold lower with unpolymerized tubulin than with MTs at pH 8.7 and 10-fold lower at pH 6.8 (Figure 6). Apparent K_m values could not be determined in all cases. Indeed, at pH 8.7, rapid MT depolymerization was observed below 0.2 μM, and at pH 6.8, a very low level of incorporation was measured with free tubulin as the substrate. Nevertheless, the apparent K_m value determined for free tubulin at pH 8.7 (∼0.3 μM) was not significantly different from that of MTs at pH 6.8 (∼0.2 μM). Thus, preferential activity toward MTs relies mainly on variations of the catalytic efficiency.

Mechanism of Glutamate Addition. Tubulin displaying polyglutamyl side chains of various lengths from one to six or seven units was previously documented (*10*, *29*−*31*). Two mechanisms, modular or sequential, can be proposed for the polyglutamylation reaction. In a modular mechanism, the modification would occur through two steps involving distinct enzymatic activities: the first one responsible for the formation of polyglutamyl chains of variable lengths and the second one for their transfer onto unglutamylated tubulin. In the case of a sequential mechanism, glutamate would be added directly onto tubulin and progressive lengthening of the side chain would be achieved by successive glutamate additions. To distinguish between these two mechanisms, we compared the glutamylation products obtained with MTs prepared either from adult mouse brain or from HeLa cells. HeLa tubulin is mostly unglutamylated and contains only low levels of monoglutamylated α- and β-tubulin, whereas adult brain tubulin is highly glutamylated, displaying side chains of various lengths ranging from one to six or seven glutamyl units. Two-dimensional PAGE patterns of these two tubulin species are presented in panels A and B of Figure 7, respectively.

The reactions were performed at limiting glutamate concentrations (13 μM ≪ K_m). With HeLa MTs, labeled prod-

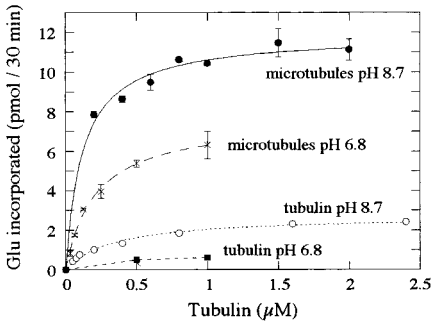

FIGURE 6: MTs are preferred substrates for tubulin polyglutamylase. Fraction IV (40 μg/mL) was assayed under standard conditions at pH 8.7 for 30 min (3 mM [^{3}H]glutamate) or at pH 6.8 for 3 h (6 mM [^{3}H]glutamate), in the presence of various concentrations of either taxotere-stabilized MTs or unpolymerized tubulin. In the latter case, taxotere was not added to the reaction mixture. Results are expressed as means ± standard deviations (n = 2) of picomoles of glutamate incorporated into α- and β-tubulin (40 μL reaction mixture) in 30 min. In the case of tubulin, standard deviations (≤7%) are not shown on the curve. At all MT concentrations tested, incorporation into α-tubulin was 2.5−3-fold higher than that into β-tubulin. Because of the low radioactivity obtained with unpolymerized tubulin, the two subunits were counted together and the α/β ratio was not determined.

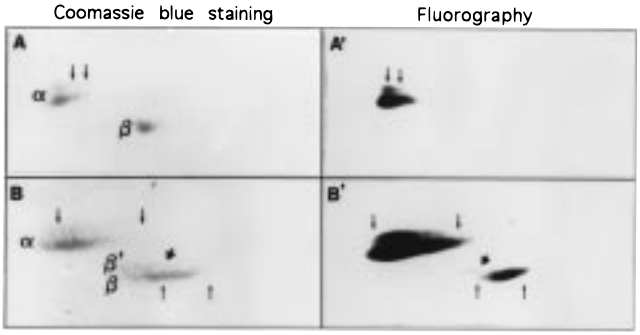

FIGURE 7: Two-dimensional PAGE analysis of in vitro-glutamylated brain and HeLa tubulin. Taxotere-stabilized MTs purified from HeLa cells (A) and from mouse brain (B) were assayed with fraction V (20 μg/mL) under standard conditions at pH 8.7 at the limiting glutamate concentration (13 μM, 1.1 × 10^{17} dpm/mol). Gels were exposed for 3 days (A′) and 10 days (B′). Arrows denote the position of the labeled α- and β-tubulin isoforms. Tubulin isoforms are shifted to the right proportionally to the length of the acidic polyglutamyl side chain. As frequently reported, α-tubulin isoforms were split into two parallel arrays. β-Tubulin isoforms migrating slightly higher correspond to the class III β-tubulin and are denoted β′. Labeled β′-tubulin isoforms are indicated by sloping arrows. Only tubulin regions of the two-dimensional gels are presented (left to right, basic to acidic isoelectric focusing first dimension; and top to bottom, SDS−PAGE second dimension).

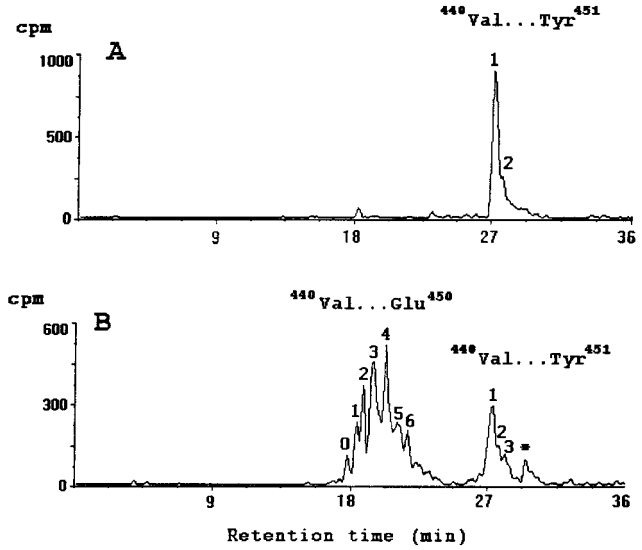

FIGURE 8: HPLC radioactive profiles of thermolysin digests of α-tubulin. Fraction V (20 μg/mL) was assayed at pH 8.7 with HeLa (A) or mouse brain (B) taxotere-stabilized MTs, in the presence of 13 μM glutamate. α-Tubulin was digested with thermolysin, and the proteolytic products were fractionated on a C18 reversed phase column. Synthetic peptides corresponding to the C-terminal sequence of α-tubulin (Val440−Glu450 and Val440−Tyr451) and containing zero to two additional glutamyl units linked to the γ-carboxylic group of Glu445 were injected simultaneously to identify the coeluting radioactive peaks. Only the radioactive profiles are shown. Numbers above each peak refer to the number of glutamyl units in polyglutamyl side chains. Note that Val440−Tyr451 peptides eluted later than Val440−Glu450 peptides and were much less resolved according to the number of glutamyl units they contain. The very minor peak numbered 0 in panel B coeluted with unglutamylated Val440−Glu450 peptide but also with Val440−Glu449 peptide bearing one glutamyl unit. It thus likely corresponds to monoglutamylated Δ2-tubulin (*22*). The peak marked with an asterisk in panel B was unidentified.

ucts were resolved into two spots migrating at the acidic side of the Coomassie blue-stained α-tubulin isoform, the first spot being largely predominant (panels A and A′ of Figure 7). Very little labeling was associated with β-tubulin (see Discussion). When analyzed by peptide mapping, this sample gave two radioactive peptides, the major one (80%) corresponding to the monoglutamylated C-terminal peptide of tyrosinated α-tubulin and the minor one (20%) corresponding to the biglutamylated species (Figure 8A). Thus, the enzyme was able to add one glutamyl unit onto unglutamylated tubulin. With MTs from adult brain, labeled α- and β-tubulin isoforms exhibited a heterogeneity similar to that of the substrate (panels B and B′ of Figure 7). Peptide mapping analysis of labeled α-tubulin products (Figure 8B) revealed a complex pattern similar to that previously observed after ex vivo glutamate labeling of cultured neurons (*32*), i.e., two series of peaks corresponding to C-terminal peptides terminating at Glu450 or Glu449 (first series) and at Tyr451 (second series). The different peaks observed within each series corresponded to peptides bearing polyglutamyl side chains of increasing length from left to right. This pattern of glutamylation could have been obtained by a modular addition onto unglutamylated tubulin, but in this case, the same products would have been expected with HeLa MTs. On the other hand, the drastically different products observed with the two kinds of MTs can be explained by addition of one glutamyl unit onto the different α-tubulin

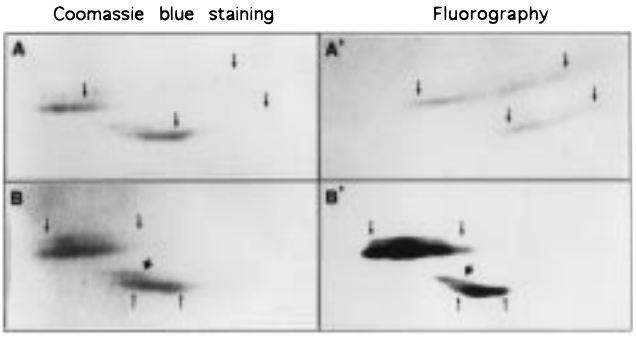

FIGURE 9: Two-dimensional PAGE analysis of glutamylated products obtained with unpolymerized and polymerized brain tubulin. Unpolymerized tubulin (A) and taxotere-stabilized MTs (B) purified from mouse brain were assayed as in Figure 7 with 2 mM glutamate. Incorporation ratios were determined in parallel: 0.1 mol of glutamate per mole of tubulin dimer in A and 0.5 in B. Gels were exposed for 1 month (A′) and 10 days (B′).

isoforms already present in each MT preparation. Taken together, these results are strongly in favor a sequential mechanism of glutamate addition.

We also compared the glutamylated products obtained with unpolymerized and polymerized brain tubulin (Figure 9). At limiting glutamate concentrations, subtle differences were observed (not shown) but they were much more evident at near-saturating glutamate concentrations. With unpolymerized tubulin, the labeling pattern showed two long stretches of α- and β-tubulin isoforms strongly shifted toward the acidic part of the gel (panels A and A′ of Figure 9). This labeling pattern could not be superimposed with that of the Coomassie blue-stained isoforms but was largely displaced beyond the hexaglutamylated position of α- and β-tubulin. This result suggests that a very minor population of the unpolymerized tubulin was extensively modified by addition of a high number of glutamyl units while the major remaining population was not modified at all. Such a behavior is strongly suggestive of a processive mechanism in which multiple additions of glutamyl units occur after a single tubulin binding event. Under the same conditions, the pattern of MT labeling remained coincident with that of the Coomassie-stained isoforms and displayed classical polyglutamyl chain lengths ranging from one to six or seven units (panels B and B′ of Figure 9). Thus, with MTs, the enzyme dissociates from the product after each cycle of glutamate addition, leading to homogeneous glutamylation of the tubulin population. In conclusion, polyglutamylation appears to be distributive with MTs and processive with unpolymerized tubulin.

DISCUSSION

Tubulin is a substrate for several posttranslational modification enzymes. Up to now, only tubulin tyrosine ligase has been purified to homogeneity and its cDNA cloned and sequenced (*33*−*35*). The enzyme that catalyzes the reverse reaction, tubulin carboxypeptidase, has been partially purified (250-fold; *36*) and tubulin acetylase 110-fold (*37*). Here, we report a ∼1000-fold purification of tubulin polyglutamylase from brains of 3-day-old mice.

Brain tissue was chosen for purifying the enzyme because of its high content in polyglutamylated tubulin. However, previous results showed that the level of posttranslational

labeling of tubulin with [^{3}H]glutamate in cultured neuronal cells decreased drastically throughout differentiation (*9*). In vitro, we observed a similar decrease of tubulin polyglutamylase activity during postnatal brain development, from newborn to adult. Whether this change is due to accumulation of a putative inhibitor or to a downregulation of tubulin polyglutamylase is not known. However, attempts to eliminate such an inhibitor by partial purification of the enzyme from 15-day-old mouse brains were unsuccessful. As use of 3-day-old mouse brain limited considerably the amount of starting material, attempts were also made to purify the enzyme from newborn sheep brain. However, specific activities of all the purified fractions were 2-fold lower than those in mouse.

The ~1000-fold purified fraction, fraction V, still contained several protein species, from which it has not been possible to identify the enzyme. In the high-molecular weight region of the SDS gel, only very faint bands were detected after silver staining. This observation suggests that the enzyme is either very minor or composed of several polypeptide chains with lower M_rs. The 110 and 130 kDa proteins prominent in fraction V appeared as two possible candidates for such enzyme subunits. However, they were not copurified with the enzyme in the following MT cosedimentation experiments. Interestingly, binding of tubulin polyglutamylase to MTs could be useful for further purification, although limited MT depolymerization occurs during the dissociation step, leading to contamination of the final supernatant with tubulin (see Figure 3B, lane 5).

Several other methods have been explored for further purification of the enzyme, including ion-exchange chromatography, isoelectric focusing in the liquid phase or with the rotofor apparatus (Bio-Rad), chromatofocusing, hydrophobic chromatography, immobilized metal-affinity chromatography (with Cu, Zn, Fe, and Co), and substrate-based (tubulin and ATP) affinity chromatography. Two types of results were obtained. (1) The enzyme did not bind to the matrix. In this case, yields were generally good but purification factors low ($\leq$1.5). (2) The enzyme seemed to bind to the matrix but was either eluted with a low yield or inativated, leading to a very low purification factor (some times $\leq$1). In isoelectric focusing experiments, the enzyme irreversibly precipitated at pH $\leq$5.5, suggesting a rather low p*I*.

Fractions IV and V were used to study the basic properties of tubulin polyglutamylase. Although one cannot exclude the presence of contaminating enzymatic activities in these fractions, care was taken to measure incorporation of glutamate into tubulin. In particular, our method of quantitation involved separation of proteins on SDS−PAGE and counting the radioactivity associated with the separated α- and β-tubulin subunits. Moreover, evidence was obtained by peptide mapping showing that the incorporated radioactivity corresponds to glutamylation.

According to the results presented here, the general scheme for the tubulin polyglutamylation reaction could be as follows:

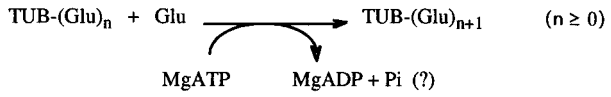

This scheme illustrates a mechanism in which the free energy generated by ATP hydrolysis serves to catalyze glutamate addition. Although the direct product of ATP hydrolysis (ADP or AMP) was not identified, MgATP was absolutely required and could not be replaced by other nucleotides. The basic mechanism is formally similar to that described for tubulin tyrosine ligase (*38*), which catalyzes addition of a tyrosine to the C terminus of detyrosylated α-tubulin, and for folylpolyglutamate synthetase (*39*), which converts folate to folylpolyglutamates, the preferred coenzyme of one-carbon metabolism.

The enzyme is very specific toward L-glutamate. For example, *N*-acetyl glutamate which is very abundant in nervous tissues or the dipeptides αGlu-Glu and γGlu-Glu were not substrates. In addition, other amino acids, in particular glycine, did not compete with glutamate, indicating that polyglutamylation and polyglycylation of tubulin are catalyzed by distinct enzymes. Interestingly, the affinity for glutamate is increased with pH up to 8.5−9, suggesting that glutamate with its deprotonated amine is the form that binds to the enzyme. However, titration of a functional group of the enzyme that plays a role in glutamate binding cannot be excluded. Comparable results were described for folylpolyglutamate synthetase (*39*). K_m(Glu), even at pH 8.7, is higher than the reported glutamate concentration in peripheral tissues (*40*); therefore, the reaction probably occurs at limiting glutamate concentrations in vivo.

Our results strongly support a sequential mechanism for glutamate addition. Whether initiation and elongation of the polyglutamyl side chains are catalyzed by one enzyme or by distinct enzymes remains to be determined. It should be noted that, although precise quantitations were not performed, the reaction rate seems not to be significantly affected by the length of the polyglutamyl chain.

Polymerized and free tubulin were not equivalent substrates for tubulin polyglutamylase. At saturating tubulin concentrations, the reaction rate with unpolymerized tubulin was ~10% of that obtained with MTs at pH 6.8 and ~25% at pH 8.7. These results demonstrate that MTs are preferred substrates and confirm previous results obtained under ex vivo conditions (*19*). Another striking difference related to the polymerization state of tubulin was observed. MTs are probably modified through a distributive mechanism in which the enzyme dissociates from tubulin after each glutamate addition, leading to a gradual lengthening of polyglutamyl side chains in the whole tubulin population. On the contrary, with free tubulin, glutamylated isoforms bearing very long side chains were obtained, whereas the vast majority of the substrate was not modified. We propose that a processive mechanism is then implicated in which multiple glutamate additions occur during a single association event between the enzyme and tubulin, the release of the product being slower than the chemical reaction. Such a behavior is common for DNA and RNA polymerases and has also been reported for the vitamin K-dependent carboxylation (*41*). Alternatively, this result could be explained by an increase of the glutamylation efficiency depending on the length of the polyglutamyl side chain. Whatever the explanation is, it is important to note that such a behavior seems to be unrelated to an artifact of in vitro conditions. Indeed, tubulin isoforms bearing very long polyglutamyl side chains have been detected in vivo. For instance, 5% of the α-tubulin present in the basal apparatus from the green flagellate *Spermatozopsis similis* carry a polyglutamyl side chain

Table 2: C-Terminal Sequences and Polyglutamylation Sites of Mouse α- and β-Tubulin Isotypes

isotype[a]	C-terminal sequence[b]	reference[c]
	437	
α1	VDSVEGEG**E**EEGEEY	*(47,8)*
α2	VDSVEGEG**E**EEGEEY	*(47,8)*
α4	IDSYE*D*EDEGEE*	*(52)*
α6	ADSAEGDD*****EGEEY	*(52)*
α3/7	VDSVEAEA*EEGEEY	*(52)*
pRDαTT1	MGSVEAEGEEEDRDTSCCIMFSSSIGNRHPC	*(52)*
	431	
β5 (class I)	EEEEDFGEE*A**E**EE*A	*(47,**54**)*
β2 (class II)	DEQG**E**FEEEEGEDE*A	*(47, **30**, **31**)*
β6 (class III)	EEEGEMY**E**DDDEESERQGPK	*(55, **10**)*
β4 (class IVa)	*EEG**E**FEEE*AEEEVA	*(47, **54**)*
β3 (class IVb)	EEEGEFEEE*AEEEVA	*(56)*
β1 (class VI)	GLEDSEEDAEEAEVEAEDKDH	*(56)*

[a] β-Tubulin isotypes are ordered according to the class number (*57*). [b] Amino acid deletions are indicated by asterisks and glutamylation sites in bold. [c] The first reference corresponds to sequences and reference(s) in bold to identification of the glutamylation site.

reaching up to 17 units (*42*), and α-tubulin side chains of 15 units were reported in *Tryponosoma brucei* (*43*). Such very acidic forms of α- and β- tubulin were also detected with the specific mAb GT335 in axonemal extracts (*16*) and exhibited two-dimensional patterns similar to those obtained after in vitro glutamylation experiments. However, hyperglutamylation was observed in vitro specifically with unpolymerized tubulin, whereas hyperglutamylated tubulin was detected in vivo in the most stable microtubular structures, e.g., axonemes. This paradox could be resolved if one hypothesizes, along with Stephens (*44*), that free or membrane-bound tubulin is transported along axonemes and assembled at their tips (*45*) and that hyperglutamylation of tubulin occurs during its transport. In nerve cells, which contain a high proportion of stable microtubules, only very low levels of hyperglutamylated α-tubulin with glutamyl side chains bearing up to 11 glutamates were recently described (*46*).

Tubulin is a highly polymorphic protein, in particular in the C-terminal region where the polyglutamylation sites are localized (Table 2). The tubulin subunits are encoded in mammals by seven different functional genes for α-tubulin and six for β-tubulin. For most of these isotypes, distinct glutamylation sites have been precisely identified. Although the C-terminal domains are very rich in glutamate residues, only one of them is concerned in each case, indicating a very high site selectivity. It appears unlikely that a single enzyme could present such a degree of selectivity toward divergent tubulin isotypes. The results obtained with HeLa and brain tubulin are consistent with the hypothesis that several isozymic forms of tubulin polyglutamylase are required for the two subunits and even for the different isotypes within each subunit. Indeed, whereas HeLa and brain α-tubulin were glutamylated at similar rates, β-tubulin from HeLa was a very poor substrate. It appears that the major α-tubulin isotypes are α1 and/or α2 (differing only in residue 232) in brain and in HeLa cells (*47*, *48*). On the other hand, class II β-tubulin is the major β-isotype expressed in brain, classes I, III, and IVa being represented to a lesser degree (*49*), whereas classe I and IVb β-isotypes are the most abundant in HeLa cells (*50*, *51*). The brain enzyme may thus contain isozymic forms which would not work on the β-tubulin isotypes expressed in HeLa cells. Further purification of the enzymatic activity and utilization of separated tubulin isotypes will be essential in further studies.

ACKNOWLEDGMENT

We are grateful to J.-C. Larcher and D. Boucher for helpful discussion and D. Guénard for providing taxotere.

REFERENCES

1. Serrano, L., Avila, J., and Maccioni, R. B. (1984) *Biochemistry 23*, 4675−4681.
2. Paschal, B. M., Obar, R. A., and Vallee, R. B. (1989) *Nature 342*, 569−572.
3. Hagiwara, H., Yorifugi, H., Sato-Yoshitake, R., and Hirokawa, N. (1994) *J. Biol. Chem. 269*, 3581−3589.
4. Boucher, D., Larcher, J. C., Gros, F., and Denoulet, P. (1994) *Biochemistry 33*, 12471−12477.
5. Larcher, J. C., Boucher, D., Lazereg, S., Gros, F., and Denoulet, P. (1996) *J. Biol. Chem. 271*, 22117−22124.
6. Sullivan, K. F. (1988) *Annu. Rev. Cell Biol. 4*, 687−716.
7. MacRae, T. H. (1997) *Eur. J. Biochem. 244*, 265−278.
8. Eddé, B., Rossier, J., Le Caer, J.-P., Desbruyères, E., Gros, F., and Denoulet, P. (1990) *Science 247*, 83−85.
9. Audebert, S., Koulakoff, A., Berwald-Netter, Y., Gros, F., Denoulet, P., and Eddé, B. (1994) *J. Cell Sci. 107*, 2313−2322.
10. Alexander, J. E., Hunt, D. F., Lee, M. K., Shabanowitz, J., Michel, H., Berlin, S. C., Macdonald, T. L., Sundberg, R. J., Rebhun, L. I., and Frankfurter, A. (1991) *Proc. Natl. Acad. Sci. U.S.A. 88*, 4685−4689.
11. Redeker, V., Le Caer, J.-P., Rossier, J., and Promé, J.-C. (1991) *J. Biol. Chem. 266*, 23461−23466.
12. Wolff, A., Houdayer, M., Chillet, D., De Néchaud, B., and Denoulet, P. (1994) *Biol. Cell 81*, 11−16.
13. Redeker, V., Rusconi, F., Mary, J., Promé, D., and Rossier, J. (1996) *J. Neurochem. 67*, 2104−2114.
14. Wolff, A., De Néchaud, B., Chillet, D., Mazarguil, H., Desbruyères, E., Audebert, S., Eddé, B., Gros, F., and Denoulet, P. (1992) *Eur. J. Cell Biol. 59*, 425−432.
15. Bré, M. H., De Néchaud, B., Wolff, A., and Fleury, A. (1994) *Cell Motil. Cytoskeleton 27*, 337−349.
16. Fouquet, J.-P., Eddé, B., Kann, M.-L., Wolff, A., Desbruyères, E., and Denoulet, P. (1994) *Cell Motil. Cytoskeleton 27*, 49−58.

17. Bobinnec, Y., Moudjou, M., Fouquet, J.-P., Desbruyères, E., Eddé, B., and Bornens, M. (1998) *Cell Motil. Cytoskeleton 39*, 223−233.
18. Gagnon, C., White, D., Cosson, J., Huitorel, P., Eddé, B., Desbruyères, E., Paturle-Lafanechère, L., Multigner, L., Job, D., and Cibert, C. (1996) *J. Cell Sci. 109*, 1545−1553.
19. Audebert, S., Desbruyères, E., Gruszczynski, C., Koulakoff, A., Gros, F., Denoulet, P., and Eddé, B. (1993) *Mol. Biol. Cell 4*, 615−626.
20. Leammli, U. K. (1970) *Nature 227*, 680−685.
21. Towbin, H., Staehelin, T., and Gordon, J. (1979) *Proc. Natl. Acad. Sci. U.S.A. 76*, 4350−4354.
22. Paturle-Lafanechère, L., Eddé, B., Denoulet, P., Dorsselaer, A. V., Mazarguil, H., Caer, J.-P. L., Wehland, J., and Job, D. (1991) *Biochemistry 30*, 10523−10528.
23. Vallee, R. V. (1982) *J. Cell Biol. 92*, 435−442.
24. Pirollet, F., Job, D., Margolis, R. L., and Garel, J. R. (1987) *EMBO J. 26*, 3247−3252.
25. Wolff, A., Denoulet, P., and Jeantet, C. (1982) *Neurosci. Lett. 31*, 323−328.
26. Denoulet, P., Jeantet, C., and Gros, F. (1982) *Biochem. Biophys. Res. Commun. 105*, 806−813.
27. Aebersold, R. H., Leavitt, J., Saavedra, R. A., Hood, L. E., and Kent, S. B. H. (1987) *Proc. Natl. Acad. Sci. U.S.A. 84*, 6970−6974.
28. Bradford, M. M. (1976) *Anal. Biochem. 72*, 248−254.
29. Eddé, B., Rossier, J., Le Caer, J.-P., Berwald-Netter, Y., Koulakoff, A., Gros, F., and Denoulet, P. (1991) *J. Cell. Biochem. 46*, 134−142.
30. Redeker, V., Melki, R., Promé, J.-C., Le Caer, J.-P., and Rossier, J. (1992) *FEBS Lett. 313*, 185−192.
31. Rüdiger, M., Plessman, U., Klöppel, K. D., Wehland, J., and Weber, K. (1992) *FEBS Lett. 308*, 101−105.
32. Eddé, B., Rossier, J., Le Caer, J.-P., Promé, J.-C., Desbruyères, E., Gros, F., and Denoulet, P. (1992) *Biochemistry 31*, 403−410.
33. Schröder, H. C., Wehland, J., and Weber, K. (1985) *J. Cell Biol. 100*, 276−281.
34. Murofushi, H. (1980) *J. Biochem. 87*, 979−984.
35. Ersfeld, K., Wehland, J., Plessmann, U., Dodemont, H., Gerke, V., and Weber, K. (1993) *J. Cell Biol. 120*, 725−732.
36. Argaraña, C. E., Barra, H. S., and Caputto, R. (1980) *J. Neurochem. 34*, 114−118.
37. Maruta, H., Greer, K., and Rosenbaum, J. L. (1986) *J. Cell Biol. 103*, 571−579.
38. Raybin, D., and Flavin, M. (1977) *Biochemistry 16*, 2189−2194.
39. Cichowicz, D. J., and Shane, B. (1987) *Biochemistry 26*, 504−512.
40. Krebs, H. E., Hems, R., and Tyler, B. (1976) *Biochem. J. 158*, 341−353.
41. Morris, D. P., Stevens, R. D., Wright, D. J., and Stafford, D. W. (1995) *J. Biol. Chem. 270*, 30491−30498.
42. Geimer, S., Tletenkötter, A., Plessmann, U., Weber, K., and Lechtreck, K.-F. (1997) *Cell Motil. Cytoskeleton 37*, 72−85.
43. Schneider, A., Plessman, U., and Weber, K. (1997) *J. Cell Sci. 110*, 431−437.
44. Stephens, R. E. (1992) *J. Cell Sci. 101*, 837−845.
45. Johnson, K. A., and Rosenbaum, J. L. (1992) *J. Cell Biol. 119*, 1605−1611.
46. Redeker, V., Rossier, J., and Frankfurter, A. (1997) *Mol. Biol. Cell 8* (Suppl.), 46a.
47. Lewis, S. A., Lee, M. G.-S., and Cowan, N. J. (1985) *J. Cell Biol. 101*, 852−861.
48. Gu, W., Lewis, S. A., and Cowan, N. J. (1988) *J. Cell Biol. 106*, 2011−2022.
49. Banerjee, A., Roach, M. C., Wall, K. A., Lopata, M. A., Cleveland, D. W., and Ludueña, R. F. (1988) *J. Biol. Chem. 263*, 3029−3034.
50. Lewis, A. L., Gilmartin, M. E., Hall, J. L., and Cowan, N. J. (1985) *J. Mol. Biol. 182*, 11−20.
51. Lewis, S. A., Gu, W., and Cowan, N. J. (1987) *Cell 49*, 539−548.
52. Villasante, A., Wang, D., Dobner, P., Dolph, P., Lewis, S. A., and Cowan, N. J. (1986) *Mol. Cell. Biol. 6*, 2409−2419.
53. Hecht, N. B., Distel, R. J., Yelick, P. C., Tanhauser, S. M., Driscoll, C. E., Goldberg, E., and Tung, K. S. K. (1988) *Mol. Cell. Biol. 8*, 996−1000.
54. Mary, J., Redeker, V., Le Caer, J. P., Promé, J. C., and Rossier, J. (1994) *FEBS Lett. 353*, 89−94.
55. Burgoyne, R. D., Cambray-Deakin, M. A., Lewis, S. A., Sarkar, S., and Cowan, N. J. (1988) *EMBO J. 7*, 2311−2319.
56. Wang, D., Villasante, A., Lewis, S. A., and Cowan, N. J. (1986) *J. Cell Biol. 103*, 1903−1910.
57. Sullivan, K. F., and Cleveland, D. W. (1986) *Proc. Natl. Acad. Sci. U.S.A. 83*, 4327−4331.

BI9804131